

Examination of competitive lanthanide sorption onto smectites and its significance in the management of radioactive waste

Evgeny Galunin (a), María D. Alba (b), Maria J. Santos (c), Taufik Abrão (b), Miquel Vidal (a)

a Departament de Química Analítica, Universitat de Barcelona, Martí i Franqués 1-11, 08028 Barcelona, Spain

b Instituto de Ciencia de Materiales de Sevilla, Consejo Superior de Investigaciones Científicas – Universidad de Sevilla, Av. Américo Vespucio 49, 41092 Sevilla, Spain

c Departamento de Química, Universidade Estadual de Londrina, Londrina, PR 86051-990, Brazil

Abstract

The competitive effect of La and Lu (analogues of radionuclides appearing in radioactive waste) in the sorption in four smectites was examined. Sorption and desorption distribution coefficients (K_d ; $K_{d,des}$), and desorption rates (R_{des}) were determined from batch tests in two media: deionized water and, to consider the influence of cement leachates, 0.02 mol L⁻¹ Ca. The competitive effect was lower when high-affinity sites were available, as in the water medium at the lowest range of initial lanthanide concentration, with high K_d for La and for Lu ($5\text{--}63 \times 10^4$ L kg⁻¹). Lower K_d was measured at higher initial concentrations and in the Ca medium, where Lu showed a stronger competitive effect. This was confirmed by fitting the sorption data to a two-solute Langmuir isotherm. The desorption data indicated that sorption was virtually irreversible for the scenarios with high sorption, with an excellent correlation between K_d and $K_{d,des}$ (R^2 around 0.9 for the two lanthanides). Assuming that radioactive waste is a mixture of radionuclides, and that Ca ions will be provided by the cement leachates, this would reduce the retention capacity of clay engineered barriers.

Keywords

Lanthanides; Sorption; Smectitic clays; Engineered barriers; Radioactive waste

1. Introduction

A deep geological repository (DGR) is the optimal storage for long-term radioactive waste management [1], [2] and [3]. Within the DGR, clay engineered barriers, usually placed between the metal canister containing the radioactive waste and external concrete barriers play a significant role in radionuclide retention. Clays have low permeability and diffusivity, high sorption capacity and strong buffering properties [4], [5] and [6]. Among the clays used for this purpose, smectites are generally considered to be the most efficient, due to their ability to

undergo strain without fracturing, their low hydraulic conductivity, high cation sorption capacity, and ability to expand and enter into close contact with both waste and rock [7]. Apart from clay engineered barriers, the DGR may include concrete bulkheads in contact with the clay backfill. Cement leachates may react with the clays, which would compromise the isolation potential of the clay and the strength of the concrete [8]. In addition, cement degradation releases alkaline calcium fluids causing geochemical transformations and modifying the clay [9] and [10]. Spent nuclear fuel contains a number of fission products, and radionuclides with high activity concentrations and long half-lives – mainly actinides and their daughter products – dominate the radiotoxicity of high-level waste [11]. To study actinide sorption–desorption processes at laboratory level, lanthanides have been used as structural and chemical analogues [12] and [13].

Factors such as pH, the nature of clay mineral interlayer cations, and ionic strength affect lanthanide sorption–desorption processes in clays [14], [15], [16] and [17]. Two main sorption mechanisms have been highlighted for lanthanides: surface complexation at the edges of the clay particles (inner-sphere interaction), and cationic exchange (outer-sphere interaction). The predominance of one mechanism over the other may depend on the lanthanide and its concentration [18], [19], [20] and [21]. Whereas some authors conclude that sorption is completely reversible [22], others suggest that it may be partially irreversible due to the strong attractive forces between trivalent lanthanide cations and clay interlayer exchange sites [23] and [24].

While there are limited data on lanthanide sorption on smectites, few authors deal with sorption studies of mixture of lanthanides, which are required to simulate scenarios for radioactive waste management. In this regard, reported data indicate that competition between the lanthanides of similar valence state and hydrolysis behavior may occur in smectites [21]. Therefore, this study aims to complete previous work on lanthanide sorption on smectites [25] and [26]. Whereas in these works the sorption–desorption pattern of lanthanides in smectites was individually evaluated with single lanthanide solutions, here we evaluate the effect of lanthanide competition on the sorption–desorption processes. As the preferential sorption–desorption mechanisms of lanthanides may vary along the lanthanide series [27] and [28], the lightest (La) and the heaviest (Lu) lanthanides were chosen to evaluate changes in the lanthanide sorption over a range of lanthanide concentration ratios. Two sorption media with different Ca concentrations were also tested to simulate the DGR conditions. The smectites examined here include hectorite, Otay montmorillonite, and MX80 and FEBEX bentonites, which are either candidates for clay engineered barriers, or already in use in experiments dealing with radioactive waste repositories. Sorption data were also fitted with two-solute Langmuir equation to facilitate comparison of the scenarios examined.

2. Materials and methods

2.1. Clay samples

Four smectites (FEBEX bentonite – FEBEX; hectorite – HEC; MX80 bentonite – MX80, and Otay montmorillonite – SCa-3) were used. Table 1 summarizes the main clay characteristics [29], [30],

[31] and [32]. These clays are 2:1 phyllosilicates and consist of layers made up by the condensation of a central octahedral sheet and two tetrahedral sheets, one on each side. Octahedral compositions depend on the octahedral occupancy, which can either be a full occupancy of the sheet if the cations are Mg (trioctahedral clays – HEC) or an occupancy of two-thirds of the available positions if the cations are Al (dioctahedral clays – FEBEX, MX80, SCa-3). In all the samples, the <2 μm -fraction was obtained, and the carbonates and organic matter were eliminated in order to ensure purity.

2.2. Sorption–desorption experiments

Batch sorption tests were carried out in 50 mL centrifuge tubes, with equilibration of 0.2 g of clay with 30 mL of the solutions that contained the mixture of lanthanides at a given concentration in two ionic media: deionised water (Milli-Q Reagent Water System from Millipore, resistivity of $>18 \text{ M}\Omega \text{ cm}^{-1}$) and $0.02 \text{ mol L}^{-1} \text{ Ca}$ ($\text{Ca}(\text{NO}_3)_2$) from Prolabo, RP Normapur, analytical grade) at an initial pH of 7. Lanthanide solutions were prepared from $\text{La}(\text{NO}_3)_3$ and $\text{Lu}(\text{NO}_3)_3$ (99.9%, Aldrich). Table 2 shows the concentrations of the theoretical initial La and Lu concentrations used in the mixture solutions. The experimental design provided the sorption isotherms of a target lanthanide at two concentration ranges and at two concentrations of the competitive lanthanide. The solutions were equilibrated with the clay samples by end-over-end shaking at 30 rpm at room temperature for 24 h. The final suspensions were centrifuged at 10,000 rpm for 25 min (Hettich Universal 30 F, with a rotor E1174) and filtered (Whatman 41, $0.22 \mu\text{m}$). The supernatants were collected in polyethylene bottles, diluted with 1% HNO_3 and stored at 4°C until analysis.

Batch desorption tests were performed the day after the sorption tests, by bringing the clay residues from the sorption tests into contact with the two ionic media mentioned above, but without the lanthanide. The other experimental conditions were as described for the sorption tests.

2.3. Scanning electron microscopy (SEM) and energy dispersion X-ray (EDX) analyses.

The morphology of the samples resulting from the sorption experiments was analyzed by a Scanning Electron Microscope using JEOL equipment (Model JSM 5400) at 20 kV. An energy dispersive X-ray (EDX) system (Oxford Link ISIS) was fitted to the SEM equipment to perform chemical analysis of the samples using a Si/Li detector with a Be window.

2.4. Determination of La and Lu in the solutions derived from sorption experiments

Lanthanide concentrations in the initial solutions and in the supernatants were analyzed by ICP-OES (Perkin–Elmer Optima-3200RL) for the concentration range over 1.5 meq L^{-1} , and by ICP-MS (Perkin–Elmer Elan-6000) for lower concentrations. The wavelengths (nm) used in the ICP-OES measurements were 384.902 (La) and 261.542 (Lu), which corresponded to the ^{139}La and ^{175}Lu isotopes in the ICP-MS measurements. Calibration curves were prepared in 1% HNO_3 , using ^{103}Rh as an internal standard, with a concentration of $10 \mu\text{g L}^{-1}$, to correct instabilities in the ICP-MS measurements. Concentration ranges of the standards were $0.05\text{--}100 \text{ mg L}^{-1}$ for La and $0.01\text{--}100 \text{ mg L}^{-1}$ for Lu). The detection limit for the ICP-OES is $50 \mu\text{g L}^{-1}$ for La and $10 \mu\text{g L}^{-1}$ for Lu, and for the ICP-MS is 5 ng L^{-1} for both lanthanides.

2.5. Calculation of sorption–desorption parameters

From the sorption–desorption tests, and following ICP-OES and ICP-MS measurements, we calculated the initial lanthanide concentration (C_{init} , meq L⁻¹), the equilibrium concentration in the supernatant after sorption experiments (C_{eq} , meq L⁻¹), and the equilibrium concentration in the supernatant after desorption experiments ($C_{eq,des}$, meq L⁻¹). Based on these data, the following parameters, required to examine lanthanide sorption–desorption in the smectites selected, were calculated:

a) sorption distribution coefficient (K_d , L kg⁻¹):

$$K_d = \frac{(C_{init} - C_{eq})V}{C_{eq}m} \quad (1)$$

where V is the liquid phase volume, in L; and m is the clay sample weight, in kg.

b) desorption distribution coefficient ($K_{d,des}$, L kg⁻¹):

$$K_{d,des} = \frac{(C_{init} - C_{eq} - C_{eq,des})V}{C_{eq,des}m} \quad (2)$$

c) desorption rate (R_{des} , %):

$$R_{des} = \frac{C_{eq,des}}{C_{init} - C_{eq}} \times 100 \quad (3)$$

2.6. Use of the two-solute Langmuir equation to fit sorption data

The Langmuir equation was used to fit sorption data, although it makes a number of assumptions – e.g., sorption takes place at specific homogeneous sites, the sorption system is monolayer and the interactions of sorbed species are not considered; the sorption energy is constant over the entire surface [33]. When dealing with sorption data with a mixture of analytes, an extended form of the Langmuir model, as shown in Eq. (4), can be used to analyze the two-solute sorption [34] and [35]. This equation allows predictions of the concentration of solute i sorbed ($C_{sorb,i}$) in the presence of sorption-competitive solutes:

$$C_{sorb,i} = \frac{b_i K_i C_{eq,i}}{1 + \sum_{j=1}^N K_j C_{eq,j}} \quad (4)$$

where $C_{eq,i}$ is the equilibrium concentration of solute i in a mixture of N solutes, and b_i and K_i constants are empirical sorption parameters obtained from the fitting of the isotherms. b represents the maximum sorption capacity determined by the reactive surface sites in an ideal monolayer system, and K represents the bonding energy associated with a pH-dependent equilibrium constant. Here we used the two-solute Langmuir model to fit the sorption data and to plot the sorption data in three-dimensional space. The three-dimensional format adds information to that of the two-dimensional fitting, and it is only rarely applied to fit competitive sorption data [36].

2.7. Data treatment

The sorption–desorption tests were performed with 3–6 replicates, which allowed the calculation of the mean and standard deviations of the derived parameters. The sorption data fittings were made using sftool (interactive environment for fitting curves to n-dimensional data), which is included in the mathematical software Matlab 7.10.0 [37]. The fitting coefficients were taken for positive values, with confidence limits $\geq 95\%$, using non-linear least squares fitting with the Trust-region or Levenberg–Marquardt algorithm option. In all fittings, the squared correlation coefficients (R^2) were close to 1.0 with low residual mean square error (RMSE).

3. Results and discussion

3.1. Description of lanthanide sorption in competitive scenarios

Table 3, Table 4, Table 5 and Table 6 summarize the sorption data for La and Lu in the two media for all the smectites, including the lanthanide initial (Cinit (La), Cinit (Lu)) and sorbed concentrations (C_{sorb}(La), C_{sorb}(Lu)), and the resulting pH in the supernatants after the sorption. There was a general decrease in the K_d values of the lanthanides with increasing initial concentrations in the two concentration ranges tested (from 0.01 to 1 meq L⁻¹, and from 0.1 to 9 meq L⁻¹), at a constant concentration of the competitive lanthanide. Moreover, the range of the K_d values obtained within the high concentration range was lower than that obtained for the low concentration range. This trend was observed for all clays and for the two lanthanides in the two media, similarly to what was previously observed in the absence of a competitive lanthanide [26]. Changes in the K_d due to the variation of the initial lanthanide concentration were higher than those due to changes in the clays, although the K_d values in the MX80 and FEBEX bentonites were consistently the lowest and the highest in the water medium, respectively.

The medium composition influenced the K_d quantification: the K_d values in the Ca medium were systematically lower than in the water medium, with decreases that were nearly two orders of magnitude in some cases, especially when La was the target solute. The only exception was MX80 clay for the low lanthanide concentration range. The results were in agreement with the previous data reported for single sorption of La and Lu [26]. In that case, the effect of Ca on the quantification of the K_d was partially explained in terms of the potential competitive influence of the Ca ions, which tend to be sorbed at interlattice sites, and then displace the lanthanides to less specific sites, as the sorbed concentration of Ca was much higher than those of the two lanthanides [26].

In the water medium, the K_d (La) were generally higher than the K_d (Lu) in the HEC and MX80 clays, whereas the opposite was observed for the SCa-3, the FEBEX showing intermediate behavior (the K_d (La) was higher only at the lowest lanthanide concentration). This finding can be explained by the fact that Lu is a cation with a greater charge density and lower radius than La, and thus with a stronger electrostatic attraction for a ligand, which affects the ionic exchange dealing with the sorption at sites with a lower sorption affinity. The exceptions observed in clays with isomorphic substitutions in the octahedral sheets, such as MX80 and HEC, can be explained in terms of the higher electrostatic attraction between the interlayer Lu ions and the tetrahedral

sheet in tetrahedrally substituted samples than in smectites without this kind of substitution [28], [38] and [39].

In the Ca medium, the $K_d(\text{La})$ were systematically lower than the $K_d(\text{Lu})$ for all the clays, with differences up to one order of magnitude. Again, the exception was the MX80 clay, in which differences were only significant at the high concentration range.

The pH affects lanthanide sorption, since it may induce new sorption sites in clays [27]. However, the pH was not controlled in these experiments. While the initial pH in the sorption experiments in the two media differed, the resulting pH in the final contact solutions was determined by the equilibrium lanthanide concentration.

3.2. Evaluation of the lanthanide competitive effect

A rapid examination of the K_d data included in Table 3, Table 4, Table 5 and Table 6 seemed to indicate that the competitive effect of the secondary lanthanide was not constant in all the scenarios tested. For a similar change in the concentration of the secondary lanthanide, the changes in the K_d of the primary lanthanide were higher in the Ca than in the water medium. Besides, Lu showed a stronger competitive effect (thus provoking a stronger decrease in the K_d) than La in the Ca medium. To illustrate these findings, Table 7 shows the changes of the K_d of the primary lanthanide (Ln (1)) due to the changes in the concentration of the secondary lanthanide (Ln (2)) in various scenarios, expressed as the K_d ratios of the primary lanthanide. The lower the ratio, the lower the influence of the secondary, competitive lanthanide on the K_d of the primary lanthanide. These ratios show that the competitive effect of the two lanthanides were similar in the water medium, with ratios usually lower than 2. The only exception was the comparison of the K_d of the primary lanthanide at a concentration of 3 meq L^{-1} when increasing the concentration of the secondary lanthanide from 0 to 3 meq L^{-1} in the HEC smectite. In the Ca medium, the competitive effect of Lu over La was higher than the opposite with many $K_d(\text{La})$ ratios near to or higher than 3.

Higher ratios (that is, higher K_d decreases) were generally observed at high initial concentrations (i.e., 3 meq L^{-1}) and in the Ca medium, which are the cases in which the K_d of the primary lanthanide was already lower. This would indicate that the presence of a competitor would mainly affect the sorption at sites with a low lanthanide affinity, thus provoking a further decrease in the K_d of the primary lanthanide. Unless the high-affinity sites of the smectites are fully occupied, the role of the competitive element could be weak. When the sorption is governed by low-affinity sites and outer-sphere mechanisms, the presence of the competitor (like the presence of Ca) could reduce the sorption of the primary lanthanide.

We completed the examination of the competitive effects with a structural analysis of the residual products of the sorption experiments. Thus, SEM/EDX measurements were carried out to clarify the competitive sorption of lanthanum and lutetium in the scenarios studied. The results for each smectite were similar. As an example we present the EDX spectra of the FEBEX bentonite samples obtained after sorption of La/Lu mixtures at the ratios 0.09/3.1 and 3.1/0.09, in the water and the Ca medium (Fig. 1). The EDX spectra of the initial FEBEX sample (Fig. 1a,(a)) were characterized by the spectral lines $K\alpha$ of Mg, Al, Si, K, Ca and Fe, and $K\beta$ of Ca and Fe, which are the constituent elements of its framework. The Cu $K\alpha$ line is due to the sample holder. Fig.

1a,b–e show new lines due to $L\alpha$ and $L\beta$ of La and Lu, with a relative intensity in good agreement with their initial concentration. Besides, Fig. 1a,d–e (samples originated from the sorption at the Ca medium) show a higher intensity line of Ca which indicates competitive sorption of Ca when present in the medium. The enlargement of the EDX spectra between 4.0 and 8.5 keV (Fig. 1b) reveals, by comparison with the framework Fe line, that in the Ca medium the sorption of La and Lu decreased, the Ca being preferentially sorbed.

Fig. 2 shows the EDX compositional mapping of the FEBEX bentonite sample after sorption of La/Lu (0.09/3.1) in the water medium, which allows analysis of the sites governing the sorption of each lanthanide in the mixtures. Whereas the EDX mappings of the Si and Al, which are framework elements, were similar to the SEM image of the lamellar structure, the La and Lu EDX mappings were similar to those of the interlayer cations (Na, Ca and K). Therefore, the similar distribution observed for La and Lu confirmed that the sorption of these lanthanides takes place at similar sites.

3.3. Use of a modified, two-solute Langmuir equation for the fitting of the sorption data

In order to describe the competitive effect of La and Lu on the lanthanide sorption onto smectites, a three-dimensional, two-solute Langmuir equation was applied to fit the sorption data. Fig. 3 shows an example of the 3-D Langmuir fitting, and Table 8 summarizes all the fitting parameters.

The values of the b parameter, which estimates the maximum sorption capacity, were similar to or slightly higher for Lu than for La in the water medium, but much higher for Lu in the Ca medium. These b values are thus consistent with the K_d pattern variation observed in the previous section. In the latter case, the sorption isotherms in the Ca medium did not indicate a maximum sorption capacity by the clays, thus the b values overcame the CEC values of the smectite. When performing the Langmuir fitting without the data of the highest initial lanthanide concentration (data not shown), the b values for Lu in the Ca medium were closer to or lower than the smectite CEC (556, 1236, 925, and 1347 meq kg^{-1} , for the FEBEX, HEC, MX80, and SCa-3 smectites, respectively).

The K parameters were higher in the water than in the Ca medium, which was consistent with the higher K_d found in the water medium. The K_1 values, generally higher than the K_2 in the water medium, also agreed with the low competitive effect observed. Moreover, their values were close to those calculated from single lanthanide solutions [26]. In contrast, the $K_2(\text{Lu})$ were similar to or higher than $K_1(\text{La})$ in the Ca medium, and much lower than those derived from single lanthanide solutions, thus indicating that Lu is the stronger competitor in this medium.

3.4. Lanthanide sorption reversibility

Table 3, Table 4, Table 5 and Table 6 also list the desorption K_d ($K_{d,\text{des}}$) and the desorption rate (R_{des}) for both lanthanides in the smectitic clays. The two parameters were highly correlated ($R_2 = 0.996$ for La and 0.999 for Lu, in all the scenarios tested), thus both predict sorption reversibility, although from two perspectives. In the water medium and from the low values of the R_{des} the lanthanide sorption in these smectites was virtually irreversible, and the effect of

the lanthanide initial concentration and smectite was stronger than the potential effect of the competitive sorption. The results are consistent with previous reports that predict sorption irreversibility due to the strong attraction between trivalent lanthanide cations and clay interlayer exchange sites [23]. However, high R_{des} values were observed at the highest concentration of the competitor in the Ca medium, which led to R_{des} values lying within the 20–50% range for La in all cases and within the 5–10% range for Lu in most cases. Therefore, this confirms that the lanthanide sorption in the Ca medium was not only lower, but also more reversible than in the water medium.

The variation pattern of the $K_{d,des}$ was quite similar to that of the K_d . In general, the $K_{d,des}$ values increased when the initial target and competitive lanthanide concentration decreased, and were lower in the Ca medium. The $K_{d,des}$ values were consistently higher than those of K_d , and the two parameters were also highly correlated ($K_{d,des La} = 1.16 (\pm 0.02) K_{d,La} + 700 (\pm 300)$, $R^2 = 0.90$; $K_{d,des Lu} = 1.21 (\pm 0.02) K_{d,Lu} + 1100 (\pm 300)$, $R^2 = 0.92$). This indicated not only that the $K_{d,des}$ was consistently higher than the K_d , thus confirming the low sorption reversibility, but also that the $K_{d,des}$ could be predicted from the sorption data.

4. Conclusions

When lanthanide sorption is limited by high-affinity sites (thus leading to high K_d values), e.g., when the initial lanthanide concentration in the water medium is low, the competitive effect of lanthanides being sorbed at smectites in binary solutions is weaker than that attributable to lanthanide concentration or smectite type. Moreover, the sites responsible for lanthanide sorption are similar for both lanthanides. Therefore, lanthanide sorption in mixtures can be predicted from data from single solutions. However, the competitive effect occurs when the low-affinity sites govern the lanthanide sorption. This is the case in the experiments in the Ca medium or with high initial lanthanide concentration, as shown here by the major competitive effect of Lu over La. In these cases not only would the sorption be diminished, but the sorption reversibility would also increase. Implications for the management of radioactive waste can easily be deduced, since it is assumed to be a mixture of radionuclides, in the presence of Ca ions. Although the concentrations of the radioactive leachates from the waste are expected to be lower than the highest values tested here, the role of the cement leachates could decrease the retention capacity of clay engineered barriers.

Acknowledgements

This research was supported by grants from the Ministry of Education and Science of Spain (Ministerio de Educación y Ciencia de España) for the Project CTM2008-01147/TECNO, from DGICYT for the Project CTQ2007-63297, and from EC for the Project funded within the 6th Framework Programme as the HRM Activity under the Contract MRTN-CT-2006-035957. Besides, the authors would like to thank Dr. A. Padró for his technical help and assistance in the ICP-OES and ICP-MS analyses. SEM-EDX analyses were carried out at the Instituto Ciencia de los Materiales de Sevilla (CICIC).

References

[1] C. McCombie, D.L. Pentz, M. Kurzeme, I. Miller

Deep geological repositories: a safe and secure solution to disposal of nuclear wastes

GeoEng2000 – An International Conference on Geotechnical and Geological Engineering, 19–24 November 2000, Melbourne, Australia (2000) Lancaster, PA: Technomic

[2] J. Astudillo Pastor

El Almacenamiento Geológico Profundo de Los Residuos Radiactivos de Alta Actividad

Principios Básicos y Tecnología, ENRESA, Madrid (2001)

[3] N. Chapman

Geological disposal of radioactive waste – concept, status and trends

J. Iber. Geol., 32 (2006), pp. 7–14

[4] A. Meunier, L. Velde, L. Griffault

The reactivity of bentonites: a review. An application to clay barrier stability for nuclear waste storage

Clay Clay Miner., 33 (1998), pp. 187–196

[5] P. Landais

Advances in geochemical research for the underground disposal of high-level, long-lived radioactive waste in a clay formation

J. Geochem. Explor., 88 (2006), pp. 32–36

[6] T. Itakura, D.W. Airey, C.J. Leo, T. Payne, G.D. McOrist

Laboratory studies of the diffusive transport of Cs-137 and Co-60 through potential waste repository soils

J. Environ. Radioact., 101 (2010), pp. 723–729

[7] R. Pusch

Engineered Barriers

V. Popov, R. Pusch (Eds.), Disposal of Hazardous Waste in Underground Mines, Wessex Institute of Technology, UK (2006), pp. 35–40

[8] F. Huertas, L. Griffault, S. Leguey, J. Cuevas, S. Ramírez, R. Vigil de la Villa, J. Cobeña, C. Andrade, M.C. Alonso, A. Hidalgo, J.C. Parneix, F. Rassineux, A. Bouchet, A. Meunier, A. Decarreau, S. Petit, P. Vieillard, Effects of Cement on Clay Barrier Performance, ECOCLAY Project. Tech. Rep. F14W-CT96-0032, European Commission, Brussels, 2000.

[9] M. Villar, I. Pérez de Villar, P. Martín, M. Pelayo, A. Fernández, A. Garralón, J. Cuevas, S. Leguey, E. Caballero, F. Huertas, C. Jiménez de Cisneros, J. Linares, E. Reyes, A. Delgado, J. Fernández-Soler, J. Astudillo

The study of Spanish clays for their use as sealing materials in nuclear waste repositories: 20 years of progress

J. Iber. Geol., 32 (2006), pp. 15–36

[10] E. Ferrage, C. Tournassat, E. Rinnert, L. Charlet, B. Lanson

Experimental evidence for calcium-chloride ion pairs in the interlayer of montmorillonite. A XRD profile modeling approach

Clay Clay Miner., 53 (2005), pp. 348–360

[11] R.C. Ewing

Nuclear waste forms for actinides

Proc. Natl. Acad. Sci. U.S.A., 96 (1999), pp. 3432–3439

[12] N. Chapman, J. Smellie

Introduction and summary of the workshop: natural analogues to the conditions around a final repository for high-level radioactive waste

Chem. Geol., 55 (1986), pp. 167–173

[13] B. Buil, P. Gomez, A. Garralon, M.J. Turrero

Rare-earth elements: a tool for understanding the behavior of trivalent actinides in the geosphere

Mater. Res. Soc. Symp. Proc., 985 (2007), pp. 437–442

[14] W. Dong, X. Wang, X. Bian, A. Wang, J. Du, Z. Tao

Comparative study on sorption/desorption of radioeuropium on alumina, bentonite and red earth: effects of pH, ionic strength, fulvic acid, and iron oxides in red earth

Appl. Radiat. Isot., 54 (2001), pp. 603–610

[15] R. Kautenburger, H.P. Beck

Influence of geochemical parameters on the sorption and desorption behaviour of europium and gadolinium onto kaolinite

J. Environ. Monit., 12 (2010), pp. 1295–1301

[16] T. Missana, U. Alonso, M. García-Gutierrez, N. Albarran, T. Lopez

Experimental Study and Modeling of Uranium (VI) Sorption onto a Spanish Smectite

Sci. Basis Nucl. Waste Manag. XXXII, 1124 (2009), pp. 561–566

[17] S. Korichi, A. Bensmaili, M. Keddam

Reactive diffusion of uranium in compacted clay: evaluation of diffusion coefficients by a kinetic approach

Diff. Sol. Liq. V, 297–301 (2010), pp. 275–280

[18] F. Coppin, G. Berger, A. Bauer, S. Castet, M. Loubet

Sorption of lanthanides on smectite and kaolinite

Chem. Geol., 182 (2002), pp. 57–68

[19] M. Bradbury, B. Baeyens

Sorption of Eu on Na and Ca-montmorillonite: experimental investigations and modelling with cation exchange and surface complexation

Geochim. Cosmochim. Acta, 66 (2002), pp. 2325–2334

[20] E. Tertre, G. Berger, S. Castet, M. Loubet, E. Giffaut

Experimental sorption of Ni²⁺, Cs⁺ and Ln³⁺ onto a montmorillonites up to 150 °C

Geochim. Cosmochim. Acta, 69 (2005), pp. 4937–4948

[21] M. Bradbury, B. Baeyens

Modelling the sorption of Mn(II), Co(II), Ni(II), Cd(II), Eu(III), Am(III), Sn(IV), Th(IV), Np(V) and U(VI) on montmorillonites: linear free energy relationships and estimates of surface binding constants for some selected heavy metals and actinides

Geochim. Cosmochim. Acta, 69 (2005), pp. 875–892

[22] D.R. Turner, R.T. Pabalan, F.P. Beretti

Neptunium (V) sorption on montmorillonite: an experimental and surface complexation modeling study

Clay Clay Miner., 46 (1998), pp. 256–259

[23] C. Bonnot-Courtois, N. Jaffrezic-Renault

Étude des échanges entre terres rares et cations interfoliaires de deux argiles

Clay Miner., 17 (1982), pp. 409–420

[24] F. Coppin, S. Castet, G. Berger, M. Loubet

Microscopic reversibility of Sm and Yb sorption onto smectite and kaolinite: experimental evidence

Geochim. Cosmochim. Acta, 67 (2003), pp. 2515–2527

[25] E. Galunin, M.D. Alba, M.A. Avilés, M.J. Santos, M. Vidal

Reversibility of La and Lu sorption onto smectites: implications for the design of engineered barriers in deep geological repositories

J. Hazard. Mater., 172 (2009), pp. 1198–1205

[26] E. Galunin, M.D. Alba, M.J. Santos, T. Abrão, M. Vidal

Lanthanide sorption on smectitic clays in presence of cement leachates

Geochim. Cosmochim. Acta, 74 (2010), pp. 862–875

[27] Y. Takahashi, A. Tada, H. Shimizu

Distribution pattern of rare earth ions between water and montmorillonites and its relation to the sorbed species of the ions

Anal. Sci., 20 (2004), pp. 1301–1306

[28] N. Finck, M.L. Schlegel, D. Bosbach

Sites of Lu (III) sorbed to and coprecipitated with hectorite

Environ. Sci. Technol., 43 (2009), pp. 8807–8812

[29] L. Ames, L. Sand, S. Goldich

A contribution on the Hector, California bentonites deposit

Econ. Geol., 53 (1958), pp. 22–37

[30] R. Grim, G. Kulbicky

Montmorillonite: high temperature reactions and classification

Am. Miner., 46 (1961), pp. 1329–1369

[31] A. Fernandez, B. Baeyens, M. Bradbury, P. Rivas

Analysis of the porewater chemical composition of a Spanish compacted bentonite used in an engineered barrier

Phys. Chem. Earth, 29 (2004), pp. 105–118

[32] G. Montes-H, B. Fritz, A. Clement, N. Michau

Modelling of geochemical reactions and experimental cation exchange in MX-80 bentonite

J. Environ. Manage., 77 (2007), pp. 35–46

[33] D. Do

Adsorption Analysis: Equilibria and Kinetics, vol. 2 Imperial College Press-ICP, London (1998)

[34] V.C. Srivastava, I.D. Mall, Mishra

Equilibrium modelling of single and binary adsorption of cadmium and nickel onto bagasse fly ash

Chem. Eng. J., 117 (2006), pp. 79–91

[35] S. Oh, M.Y. Kwak, W.S. Shin

Competitive sorption of lead and cadmium onto sediments

Chem. Eng. J., 152 (2009), pp. 376–388

[36] C. Yan, G. Li, P. Xue, Q. Wei, Q. Li

Competitive effect of Cu(II) and Zn(II) on the biosorption of lead(II) by *Myriophyllum spicatum*

J. Hazard. Mater., 179 (2010), pp. 721–728

[37] The Mathworks Inc., User Guide – Matlab 7.10.0 (R2010a), Apple Hill Drive, Natick, MA 01760-2098, USA, 2010.

[38] G. Sposito, R. Prost

Structure of water adsorbed on smectites

Chem. Rev., 82 (1982), pp. 553–573

[39] B.J. Teppen, D.M. Miller

Hydration energy determines isovalent cation exchange selectivity by clay minerals

Soil Sci. Soc. Am. J., 70 (2006), pp. 31–40

Figure captions

Figure 1. (a) EDX spectra of the FEBEX smectite: a) initial sample, b) after sorption of La/Lu (0.09/3.1) in the water medium, c) after sorption of La/Lu (3.1/0.09) in the water medium, d) after sorption of La/Lu (0.09/3.1) in the Ca medium and e) after sorption of La/Lu (3.1/0.09) in the Ca medium. (b) Enlargement of the EDX spectra of the FEBEX smectite in the 4–8.5 keV range: a) after sorption of La/Lu (0.09/3.1) in the water medium, b) after sorption of La/Lu (3.1/0.09) in the water medium, c) after sorption of La/Lu (0.09/3.1) in the Ca medium and d) after sorption of La/Lu (3.1/0.09) in the Ca medium.

Figure 2. SEM micrograph and EDX mapping of the FEBEX smectite after sorption of La/Lu (0.09/3.1) in the water medium. The scale mark in the EDX mappings indicates 1 μm .

Figure 3. Fitting of the sorption data with the three-dimensional, two-solute Langmuir equation. Case of the HEC smectite. Prediction of the $C_{\text{orb,La}}$ (a) and $C_{\text{orb,Lu}}$ (b) in the water medium, and of the $C_{\text{orb,La}}$ (c) and $C_{\text{orb,Lu}}$ (d) in the Ca medium.

Table 1

Table 1. Characteristics of smectitic clays selected for sorption experiments.

Clay	Structural formula	Geometry	Isomorphic substitutions	Total charge/u.c.	CEC meq kg ⁻¹ ^e	pH
FEBEX ^a	(Ca _{0.5} Na _{0.08} K _{0.11}) (Si _{7.78} Al _{0.22}) (Al _{2.78} Fe ^{III} _{0.33} Fe ^{II} _{0.02} Mg _{0.81}) O ₂₀ (OH) ₄	Diocahedral	Tetrahedral and octahedral sheets	1.19	1582	9.6
HEC ^b	Ca _{0.33} (Si _{7.96} Al _{0.04}) (Mg _{5.3} Al _{0.04} Li _{0.66}) O ₂₀ (OH) ₄	Triocahedral	Octahedral sheet	0.66	871	10.4
MX80 ^c	(Na _{0.36} Ca _{0.20}) (Si _{7.96} Al _{0.04}) (Al _{3.1} Mg _{0.56} Fe ^{III} _{0.18} Fe ^{II} _{0.16}) O ₂₀ (OH) ₄	Diocahedral	Octahedral sheet	0.76	1021	7.6
SCa-3 ^d	(Mg _{0.45} Ca _{0.15} Na _{0.26} K _{0.01}) {Si _{7.81} Al _{0.19} } {Al _{2.55} Mg _{1.31} Fe _{0.12} Ti _{0.02} } O ₂₀ (OH) ₄	Diocahedral	Tetrahedral and octahedral sheets	1.47	1979	9.0

a Bentonite FEBEX (ENRESA, Spain).

b Hectorite (Source Clays Repository of the Clay Minerals Society, University of Missouri, Columbia, USA).

c Bentonite MX80 (CIEMAT, Spain).

d Otay montmorillonite (Solvay Alkali GMBH).

e Theoretical cation exchange capacity value, mathematically deduced from clay molecular formula.

Table 2

Table 2. Experimental design: theoretical initial La and Lu concentrations ($C_{init,La}$, $C_{init,Lu}$; meq L⁻¹) in the mixture solutions.

La sorption isotherms		Lu sorption isotherms	
$C_{init,La}$	$C_{init,Lu}$	$C_{init,Lu}$	$C_{init,La}$
0	0.03	0	0.03
0.01	0.03	0.01	0.03
0.03	0.03	0.03	0.03
0.09	0.03	0.09	0.03
1	0.03	1	0.03
0	3	0	3
0.09	3	0.09	3
1	3	1	3
3	3	3	3
9	3	9	3

Table 3

Table 3. Sorption–desorption parameters for both lanthanides in the tested clays in the water medium (C_{init} , meq L⁻¹; C_{sorb} , meq kg⁻¹; K_d (SD), $K_{d,des}$ (SD), L kg⁻¹; R_{des} (SD), %).

Clay	pH	C_{init} (La)	C_{init} (Lu)	C_{sorb} (La)	C_{sorb} (Lu)	La			Lu		
						K_d	$K_{d,des}$	R_{des}	K_d	$K_{d,des}$	R_{des}
FEBEX	9.0	0	0.03	–	4.8	–	–	–	32,900 (1400)	35,100 (300)	0.5 (0.1)
	9.7	0.01	0.03	1.4	4.9	63,400 (1300)	64,200 (900)	0.2 (0.1)	33,800 (2100)	44,900 (5500)	0.3 (0.1)
	9.7	0.03	0.03	4.5	4.7	28,000 (2700)	30,400 (450)	0.5 (0.1)	32,700 (2800)	41,100 (7700)	0.4 (0.1)
	9.5	0.09	0.03	14	4.9	26,100 (1500)	27,000 (600)	0.6 (0.1)	26,000 (3400)	29,200 (4300)	0.5 (0.1)
	8.7	1.01	0.04	150	5.4	23,200 (600)	26,500 (1100)	0.6 (0.1)	22,600 (2200)	26,700 (2900)	0.5 (0.1)
	6.5	0	3.03	–	450	–	–	–	15,900 (1600)	20,400 (260)	0.8 (0.1)
	6.7	0.10	3.06	14	450	16,100 (1100)	19,500 (2200)	0.8 (0.1)	14,100 (1300)	15,800 (720)	1.0 (0.1)
	6.7	1.20	3.15	180	460	14,900 (1200)	15,400 (550)	1.0 (0.2)	13,000 (520)	14,300 (380)	1.1 (0.1)
	6.1	3.13	3.15	470	470	11,700 (340)	12,900 (290)	1.2 (0.1)	12,700 (540)	13,900 (330)	1.1 (0.1)
	6.0	9.17	3.19	850	300	240 (20)	11,300 (240)	1.3 (0.1)	250 (10)	6200 (70)	2.4 (0.1)
HEC	10.1	0	0.03	–	4.8	–	–	–	16,300 (2400)	53,000 (5700)	0.3 (0.1)
	10.4	0.01	0.03	1.4	4.9	31,700 (670)	59,300 (8000)	0.3 (0.1)	14,000 (1800)	20,000 (1100)	0.8 (0.1)
	10.4	0.03	0.03	4.6	4.8	28,400 (2600)	33,700 (4100)	0.5 (0.1)	13,700 (1900)	16,300 (870)	1.0 (0.1)
	10.3	0.09	0.03	14	4.9	28,100 (1900)	35,800 (2300)	0.4 (0.1)	12,400 (450)	15,300(170)	1.0 (0.1)
	9.8	1.01	0.04	150	5.4	22,100 (3200)	23,700 (3300)	0.7 (0.1)	12,100 (80)	14,500 (180)	1.1 (0.1)
	7.1	0	3.03	–	450	–	–	–	10,000 (1100)	16,300 (480)	1.0 (0.1)
	7.4	0.10	3.06	14	450	14,500 (1500)	18,800 (1600)	0.8 (0.1)	7300 (510)	9300 (120)	1.6 (0.1)

Clay	pH	C _{init} (La)	C _{init} (Lu)	C _{sorb} (La)	C _{sorb} (Lu)	La			Lu		
						K _d	K _{d,des}	R _{des}	K _d	K _{d,des}	R _{des}
	7.1	1.20	3.15	170	450	13,800 (1300)	14,900 (850)	1.0 (0.1)	5500 (180)	7800 (90)	1.9 (0.1)
	6.7	3.13	3.15	440	460	1200 (50)	8800 (440)	1.8 (0.1)	1500 (50)	6700 (90)	2.3 (0.1)
	6.4	9.17	3.19	600	310	120 (1)	3400 (280)	4.2 (0.4)	274 (0)	3500 (100)	4.2 (0.2)
MX80	9.9	0	0.03	–	4.7	–	–	–	4400 (350)	6800 (1300)	2.4 (0.4)
	9.9	0.01	0.03	1.3	4.7	8300 (820)	10,600 (70)	1.5 (0.1)	5000 (390)	5700 (570)	2.7 (0.3)
	9.9	0.03	0.03	4.4	4.5	6500 (760)	7600 (630)	2.0 (0.2)	4300 (250)	5300 (460)	2.9 (0.2)
	9.9	0.09	0.03	14	4.7	5000 (1400)	6300 (1600)	2.5 (0.5)	4100 (5)	5000 (30)	3.0 (0.1)
	9.0	1.01	0.04	150	5.4	2800 (210)	3500 (220)	4.3 (0.1)	3900 (170)	4200 (190)	3.6 (0.3)
	7.2	0	3.03	–	440	–	–	–	3100 (140)	4000 (550)	3.9 (0.5)
	7.5	0.10	3.06	14	460	3300 (220)	4000 (560)	3.9 (0.5)	5900 (8)	7200 (120)	2.1 (0.1)
	7.2	1.20	3.15	170	460	2900 (130)	3700 (240)	4.0 (0.2)	4100 (330)	4700 (160)	3.2 (0.1)
	6.7	3.13	3.15	440	440	2900 (130)	3600 (280)	4.0 (0.3)	2200 (60)	2700 (80)	5.2 (0.1)
	6.3	9.17	3.19	700	270	160 (4)	2700 (500)	5.2 (0.9)	210 (7)	1800 (110)	7.7 (0.5)
SCa-3	8.9	0	0.03	–	4.6	–	–	–	48,500 (5500)	49,900 (6200)	0.3 (0.1)
	9.1	0.01	0.03	1.4	4.9	23,100 (5300)	57,300 (11,700)	0.3 (0.1)	44,500 (6000)	73,500 (1300)	0.2 (0.1)
	9.2	0.03	0.03	4.7	4.9	22,800 (2900)	24,800 (2100)	0.6 (0.1)	30,200 (3900)	39,900 (4)	0.4 (0.1)
	9.0	0.09	0.03	14	4.8	21,700 (1400)	24,400 (1600)	0.6 (0.1)	28,200 (4300)	27,900 (2300)	0.6 (0.1)
	7.7	1.01	0.04	150	5.3	21,200 (2000)	23,400 (1800)	0.7 (0.1)	17,200 (1500)	20,600 (3000)	0.8 (0.1)
	6.5	0	3.03	–	450	–	–	–	27,000 (2000)	28,700 (480)	0.6 (0.1)
	6.6	0.10	3.06	14	460	18,200 (1700)	20,600 (2500)	0.7 (0.1)	26,400 (3100)	29,700 (2400)	0.5 (0.1)

Clay	pH	C_{init} (La)	C_{init} (Lu)	C_{sorb} (La)	C_{sorb} (Lu)	La			Lu		
						K_d	$K_{d,des}$	R_{des}	K_d	$K_{d,des}$	R_{des}
	7.1	1.20	3.15	180	470	16,800 (960)	20,000 (820)	0.8 (0.1)	21,400 (960)	25,900 (1400)	0.6 (0.1)
	6.5	3.13	3.15	470	470	12,000 (190)	13,800 (210)	1.1 (0.1)	10,700 (920)	12,600 (380)	1.2 (0.1)
	6.0	9.17	3.19	1000	370	450 (20)	4100 (60)	3.5 (0.1)	530 (20)	2500 (210)	5.6

Table 4

Table 4. Sorption–desorption parameters for both lanthanides in the tested clays in the water medium (C_{init} , meq L⁻¹; C_{sorb} , meq kg⁻¹; K_d (SD), $K_{d,des}$ (SD), L kg⁻¹; R_{des} (SD), %).

Clay	pH	C_{init} (Lu)	C_{init} (La)	C_{sorb} (Lu)	C_{sorb} (La)	Lu			La		
						K_d	$K_{d,des}$	R_{des}	K_d	$K_{d,des}$	R_{des}
FEBEX	9.2	0	0.03	–	4.6	–	–	–	23,800 (3100)	44,900 (490)	0.4 (0.1)
	9.9	0.01	0.03	1.5	4.3	43,000 (780)	43,800 (760)	0.3 (0.1)	28,500 (500)	33,900 (590)	0.4 (0.1)
	9.7	0.03	0.03	4.7	4.5	32,700 (2800)	41,100 (7700)	0.4 (0.1)	28,000 (2700)	30,400 (450)	0.5 (0.1)
	9.7	0.09	0.03	14	4.5	25,700 (3900)	27,900 (3100)	0.5 (0.1)	14,400 (810)	16,400 (1600)	0.9 (0.1)
	7.4	1.15	0.03	170	5.0	15,400 (3900)	16,900 (500)	0.9 (0.1)	8100 (650)	10,900 (1100)	1.4 (0.1)
	6.6	0	3.29	–	490	–	–	–	15,100 (550)	24,600 (1500)	0.6 (0.1)
	7.1	0.09	3.10	14	470	13,600(2000)	15,500 (2500)	1.0 (0.2)	22,000 (1600)	23,900 (1700)	0.6 (0.1)
	6.7	1.08	3.13	160	470	13,600 (680)	15,300 (580)	1.0 (0.1)	15,700 (930)	18,300 (970)	0.8 (0.1)
	6.1	3.15	3.13	470	470	12,700 (540)	13,900 (330)	1.1 (0.1)	11,700 (340)	12,900 (290)	1.2 (0.1)
	6.0	9.12	3.10	820	290	220 (10)	9800 (480)	1.5 (0.1)	240 (20)	5200 (610)	2.9 (0.4)
HEC	10.2	0	0.03	–	4.6	–	–	–	50,100 (5700)	114,000 (2500)	0.2 (0.1)
	10.4	0.01	0.03	1.5	4.3	14,700 (3600)	29,500 (610)	0.5 (0.1)	31,000 (3700)	34,500 (640)	0.4 (0.1)
	10.4	0.03	0.03	4.8	4.6	13,700 (1900)	16,300 (870)	1.0 (0.1)	28,400 (2600)	33,700 (4100)	0.5 (0.1)
	10.4	0.09	0.03	14	4.6	12,600 (810)	15,200 (1100)	1.1 (0.1)	24,200 (3800)	26,600 (2000)	0.6 (0.1)
	9.6	1.15	0.03	170	4.8	5100 (290)	4600 (390)	3.2 (0.3)	2900 (330)	3100 (380)	4.8 (0.6)
	8.7	0	3.29	–	490	–	–	–	25,100 (1100)	28,600 (900)	0.5 (0.1)
	9.0	0.09	3.10	14	470	10,200 (460)	12,000 (630)	1.3 (0.1)	24,300 (580)	26,500 (650)	0.6 (0.1)

Clay	pH	C _{init} (Lu)	C _{init} (La)	C _{sorb} (Lu)	C _{sorb} (La)	Lu			La		
						K _d	K _{d,des}	R _{des}	K _d	K _{d,des}	R _{des}
	7.3	1.08	3.13	160	460	3600 (350)	9400 (510)	1.6 (0.1)	9700 (980)	11,700 (440)	1.3 (0.1)
	6.7	3.15	3.13	460	440	1500 (50)	6700 (90)	2.3 (0.1)	1200 (50)	8800 (440)	1.8 (0.1)
	6.2	9.12	3.10	690	210	150 (60)	6100 (1700)	2.5 (0.7)	120 (50)	1900 (870)	8 (3)
MX80	9.8	0	0.03	–	4.6	–	–	–	6600 (160)	9600 (530)	1.6 (0.1)
	10.0	0.01	0.03	1.5	4.3	5200 (680)	6100 (890)	2.6 (0.4)	6800 (800)	9600 (990)	1.8 (0.2)
	9.9	0.03	0.03	4.5	4.4	4300 (250)	5300 (460)	2.9 (0.2)	6500 (760)	7600 (630)	2.0 (0.2)
	9.9	0.09	0.03	13	4.5	3300 (400)	3900 (670)	3.8 (0.6)	6100 (90)	7200 (400)	2.1 (0.2)
	8.7	1.15	0.03	160	4.9	3000 (80)	3700 (110)	4.0 (0.2)	5700 (20)	6300 (280)	2.4 (0.1)
	7.5	0	3.29	–	480	–	–	–	5000 (200)	7000 (180)	2.1 (0.1)
	7.6	0.09	3.10	13	450	2500 (290)	3000 (340)	5.0 (0.6)	5300 (460)	6300 (150)	2.4 (0.1)
	7.3	1.08	3.13	150	460	2300 (180)	2800 (120)	5.3 (0.3)	4500 (130)	5200 (120)	2.9 (0.1)
	6.7	3.15	3.13	440	440	2200 (60)	2700 (80)	5.2 (0.1)	2900 (130)	3600 (280)	4.0 (0.3)
	6.2	9.12	3.10	750	260	180 (20)	2400 (160)	5.9 (0.4)	180 (20)	810 (100)	16 (2)
SCa-3	8.9	0	0.03	–	6.1	–	–	–	33,000 (2400)	73,000 (4100)	0.2 (0.1)
	8.9	0.01	0.03	1.5	4.4	33,600 (4200)	44,700 (670)	0.3 (0.1)	23,800 (2400)	29,600 (440)	0.5 (0.1)
	9.2	0.03	0.03	4.9	4.7	30,200 (3900)	39,900 (4)	0.4 (0.1)	22,800 (2900)	24,800 (2100)	0.6 (0.1)
	9.0	0.09	0.03	14	4.6	26,700 (2200)	36,000 (3200)	0.4 (0.1)	18,100 (2300)	21,900 (70)	0.7 (0.1)
	7.6	1.15	0.03	170	5.1	25,000 (2500)	32,200 (1700)	0.5 (0.1)	14,300 (2100)	19,400 (3500)	0.8 (0.1)
	6.5	0	3.29	–	500	–	–	–	12,800 (1000)	38,800 (1900)	0.4 (0.1)
	6.9	0.09	3.10	14	450	20,800 (850)	25,100 (2800)	0.6 (0.1)	14,500 (560)	17,500 (1100)	0.9 (0.1)

Clay	pH	C_{init} (Lu)	C_{init} (La)	C_{sorb} (Lu)	C_{sorb} (La)	Lu			La		
						K_d	$K_{d,des}$	R_{des}	K_d	$K_{d,des}$	R_{des}
	6.8	1.08	3.13	160	460	20,000 (2100)	23,000 (2200)	0.6 (0.1)	12,900 (1000)	15,200 (680)	1.0 (0.1)
	6.5	3.15	3.13	470	470	10,700 (920)	12,600 (380)	1.2 (0.1)	12,000 (190)	13,800 (210)	1.1 (0.1)
	5.9	9.12	3.10	1000	350	430 (10)	6000 (220)	2.5 (0.1)	460 (10)	2300 (300)	6.5 (0.6)

Table 5

Table 5. Sorption–desorption parameters for both lanthanides in the tested clays in the Ca medium (C_{init} , meq L⁻¹; C_{sorb} , meq kg⁻¹; K_d (SD), $K_{d,des}$ (SD), L kg⁻¹; R_{des} (SD), %).

Clay	pH	C_{init} (La)	C_{init} (Lu)	C_{sorb} (La)	C_{sorb} (Lu)	La			Lu		
						K_d	$K_{d,des}$	R_{des}	K_d	$K_{d,des}$	R_{des}
FEBEX	7.3	0	0.03	–	3.9	–	–	–	13,200 (2700)	13,400 (1200)	1.2 (0.1)
	7.3	0.01	0.03	1.5	4.5	1700 (180)	2800 (400)	5.1 (0.7)	7800 (770)	9100 (70)	1.6 (0.1)
	7.3	0.03	0.03	4.1	4.2	1700 (110)	2000 (20)	7.3 (0.1)	6400 (370)	8500 (710)	1.8 (0.1)
	7.2	0.09	0.03	12	4.4	1100 (100)	1500 (220)	9.7 (0.9)	4900 (150)	5900 (230)	2.6 (0.2)
	6.5	1.20	0.04	150	5.6	700 (10)	990 (70)	14 (1)	4000 (180)	4300 (360)	3.5 (0.3)
	6.8	0	2.95	–	400	–	–	–	1400 (200)	1900 (300)	7.0 (1.0)
	6.3	0.10	3.17	11	410	420 (30)	470 (10)	24 (1)	840 (50)	1900 (140)	7.6 (0.5)
	6.4	1.13	3.07	120	380	360 (30)	460 (30)	25 (1)	750 (30)	1500 (80)	9.2 (0.4)
	6.5	2.93	3.12	260	380	220 (–)	210 (5)	41 (2)	710 (1)	980 (20)	13 (1)
	6.2	9.01	3.01	620	250	130 (1)	200 (20)	43 (2)	190 (2)	550 (20)	22 (2)
HEC	7.9	0	0.03	–	3.9	–	–	–	13,700 (1200)	14,700 (440)	0.7 (0.1)
	8.2	0.01	0.03	1.5	4.6	2200 (430)	3000 (780)	5.2 (0.9)	12,000 (1100)	14,800 (610)	1.0 (0.1)
	8.4	0.03	0.03	4.1	4.2	1600 (190)	1900 (90)	7.3 (0.3)	9100 (550)	11,500 (390)	1.3 (0.1)
	8.4	0.09	0.03	12	4.4	1300 (100)	1700 (270)	8.2 (0.9)	8800 (40)	10,200 (170)	1.5 (0.1)
	6.7	1.20	0.04	130	5.6	350 (20)	1200 (50)	11 (1)	8500 (–)	9700 (600)	1.6 (0.1)
	8.1	0	2.95	–	400	–	–	–	1100 (100)	1300 (80)	11 (1)
	6.6	0.10	3.17	8	430	200 (7)	450 (20)	25 (1)	1500 (140)	7400 (200)	2.0 (0.1)

Clay	pH	C_{init} (La)	C_{init} (Lu)	C_{sorb} (La)	C_{sorb} (Lu)	La			Lu		
						K_d	$K_{d,des}$	R_{des}	K_d	$K_{d,des}$	R_{des}
	6.5	1.13	3.07	90	410	180 (30)	420 (100)	27 (5)	1300 (60)	4700 (80)	3.1 (0.1)
	6.7	2.93	3.12	220	420	150 (3)	420 (3)	26 (1)	1200 (20)	4200 (40)	3.6 (0.1)
	6.5	9.01	3.01	370	290	60 (1)	160 (20)	46 (2)	270 (1)	760 (20)	17 (1)
MX80	8.0	0	0.03	–	3.8	–	–	–	9100 (940)	12,300 (1000)	1.2 (0.1)
	7.9	0.01	0.03	1.6	4.7	14,000 (1800)	19,100 (300)	0.8 (0.1)	15,700 (600)	16,700 (490)	0.9 (0.1)
	8.1	0.03	0.03	4.5	4.3	10,600 (490)	12,300 (1200)	1.2 (0.1)	12,800 (590)	16,300 (910)	0.9 (0.1)
	8.1	0.09	0.03	13	4.4	10,800 (520)	14,400 (1200)	1.0 (0.1)	12,000 (800)	13,400 (50)	1.1 (0.1)
	6.7	1.20	0.04	130	5.8	390 (30)	1200 (30)	11 (–)	11,400 (1300)	13,000 (1200)	1.2 (0.1)
	6.6	0	2.95	–	340	–	–	–	460 (4)	700 (20)	18 (–)
	6.5	0.10	3.17	11	390	500 (30)	490 (40)	24 (2)	740 (20)	3300 (130)	4.5 (0.1)
	6.4	1.13	3.07	100	380	230 (40)	320 (60)	32 (4)	650 (40)	2700 (130)	5.4 (0.2)
	6.5	2.93	3.12	250	380	200 (5)	320 (6)	32 (2)	620 (20)	1200 (20)	11 (1)
	6.3	9.01	3.01	440	220	70 (1)	140 (1)	51 (3)	140 (1)	470 (2)	24 (2)
SCa-3	7.1	0	0.03	–	3.8	–	–	–	11,200 (990)	12,200 (2200)	1.2 (0.2)
	7.7	0.01	0.03	1.6	4.6	5100 (270)	5900 (360)	2.6 (0.1)	18,100 (1800)	25,200 (3300)	0.6 (0.1)
	7.6	0.03	0.03	4.4	4.3	4800 (540)	5200 (20)	2.9 (0.1)	13,600 (1700)	18,100 (2200)	0.8 (0.1)
	7.3	0.09	0.03	13	4.4	3100 (420)	4000 (750)	3.8 (0.7)	11,300 (890)	13,000 (1200)	1.2 (0.1)
	6.6	1.20	0.04	160	5.7	870 (10)	1400 (50)	10 (1)	10,600 (1300)	12,600 (910)	1.2 (0.1)
	6.5	0	2.95	–	380	–	–	–	850 (90)	1800 (35)	12 (1)
	6.4	0.10	3.17	12	440	610 (30)	570 (30)	21 (1)	1600 (50)	4300 (530)	3.5 (0.4)

Clay	pH	C_{init} (La)	C_{init} (Lu)	C_{sorb} (La)	C_{sorb} (Lu)	La			Lu		
						K_d	$K_{d,des}$	R_{des}	K_d	$K_{d,des}$	R_{des}
	6.3	1.13	3.07	130	420	450 (60)	510 (40)	23 (1)	1400 (60)	3100 (130)	4.8 (0.3)
	6.6	2.93	3.12	320	420	390 (20)	470 (9)	25 (2)	1200 (50)	1900 (190)	7.6 (0.5)
	6.0	9.01	3.01	700	300	160 (1)	330 (6)	31 (2)	290 (5)	860 (50)	15 (1)

Table 6

Table 6. Sorption–desorption parameters for both lanthanides in the tested clays in the Ca medium (C_{init} , meq L⁻¹; C_{sorb} , meq kg⁻¹; K_d (SD), $K_{d,des}$ (SD), L kg⁻¹; R_{des} (SD), %).

Clay	pH	C_{init} (Lu)	C_{init} (La)	C_{sorb} (Lu)	C_{sorb} (La)	Lu			La		
						K_d	$K_{d,des}$	R_{des}	K_d	$K_{d,des}$	R_{des}
FEBEX	7.3	0	0.04	–	5.6	–	–	–	3600 (760)	2900 (180)	5.1 (0.3)
	7.4	0.01	0.03	1.4	4.3	10,700 (2000)	11,400 (1200)	1.3 (0.1)	2500 (230)	2600 (310)	5.6 (0.6)
	7.3	0.03	0.03	4.2	4.1	6400 (370)	8500 (710)	1.8 (0.1)	1700 (110)	2000 (20)	7.3 (0.1)
	7.3	0.09	0.03	13	4.0	4800 (580)	6800 (840)	2.2 (0.3)	1200 (120)	1400 (80)	10 (1)
	6.4	1.27	0.04	160	4.4	880 (20)	1100 (4)	12 (1)	600 (6)	700 (40)	18 (1)
	6.6	0	2.62	–	330	–	–	–	630 (60)	670 (110)	19 (2)
	6.4	0.10	3.05	15	320	3000 (420)	4200 (380)	3.6 (0.3)	360 (20)	450 (40)	25 (1)
	6.4	1.24	2.97	160	300	770 (40)	1100 (70)	12 (1)	300 (20)	320 (20)	33 (1)
	6.5	3.12	2.93	380	260	710 (1)	980 (20)	13 (1)	220 (–)	210 (5)	41 (0)
	6.5	9.19	2.94	1100	260	500 (5)	610 (20)	20 (2)	220 (–)	200 (8)	43 (1)
HEC	7.7	0	0.04	–	5.5	–	–	–	2100 (260)	3000 (160)	5.0 (0.3)
	8.5	0.01	0.03	1.4	4.2	9300 (50)	12,100 (60)	1.2 (0.1)	2100 (150)	2200 (120)	6.4 (0.4)
	8.4	0.03	0.03	4.2	4.1	9100 (550)	11,500 (390)	1.3 (0.1)	1600 (190)	1900 (90)	7.3 (0.3)
	8.4	0.09	0.03	13	3.9	8800 (660)	9300 (300)	1.6 (0.1)	1100 (30)	1300 (170)	11 (1)
	7.1	1.27	0.04	170	4.5	1700 (8)	5000 (270)	3.0 (0.1)	640 (50)	670 (100)	19 (2)
	7.4	0	2.62	–	320	–	–	–	660 (300)	640 (20)	19 (1)
	6.0	0.10	3.05	15	270	9100 (380)	10,200 (490)	1.5 (0.1)	220 (1)	1400 (230)	10 (1)

Clay	pH	C _{init} (Lu)	C _{init} (La)	C _{sorb} (Lu)	C _{sorb} (La)	Lu			La		
						K _d	K _{d,des}	R _{des}	K _d	K _{d,des}	R _{des}
	6.7	1.24	2.97	170	250	1600 (30)	4400 (190)	3.4 (0.2)	180 (6)	650 (20)	19 (1)
	6.7	3.12	2.93	420	220	1200 (20)	4200 (40)	3.6 (0.1)	150 (3)	420 (3)	26 (2)
	6.5	9.19	2.94	1100	200	470 (5)	1800 (20)	7.7 (0.1)	120 (1)	330 (4)	31 (2)
MX80	7.8	0	0.04	—	5.7	—	—	—	13,500 (1200)	24,000 (310)	0.6 (0.1)
	8.1	0.01	0.03	1.4	4.5	15,400 (1900)	28,700 (10)	0.5 (0.1)	11,200 (520)	14,100 (1400)	1.1 (0.1)
	8.1	0.03	0.03	4.3	4.5	12,800 (590)	16,300 (910)	0.9 (0.1)	10,600 (490)	12,300 (1200)	1.2 (0.1)
	8.0	0.09	0.03	13	4.4	12,000 (1500)	15,400 (1900)	1.0 (0.1)	9700 (890)	10,900 (280)	1.4 (0.1)
	6.7	1.27	0.04	170	4.4	1100 (90)	2700 (480)	5.5 (0.9)	550 (30)	710 (100)	18 (2)
	6.3	0	2.62	—	310	—	—	—	600 (20)	1400 (70)	10 (1)
	6.5	0.10	3.05	16	330	9500 (200)	11,300 (940)	1.4 (0.1)	360 (4)	680 (—)	19 (—)
	6.6	1.24	2.97	150	280	680 (20)	1600 (80)	8.6 (0.4)	260 (20)	440 (40)	26 (2)
	6.5	3.12	2.93	380	250	620 (20)	1200 (20)	11 (1)	200 (5)	320 (6)	32 (3)
	6.3	9.19	2.94	1000	220	410 (1)	750 (3)	17 (1)	150 (—)	220 (3)	40 (1)
SCa-3	7.0	0	0.04	—	5.9	—	—	—	16,600 (1700)	28,000 (550)	0.6 (0.1)
	7.6	0.01	0.03	1.5	4.4	15,500 (1900)	29,100 (440)	0.5 (0.1)	5200 (250)	6200 (500)	2.4 (0.2)
	7.6	0.03	0.03	4.3	4.4	13,600 (1700)	18,100 (2200)	0.8 (0.1)	4800 (540)	5200 (20)	2.9 (0.1)
	7.6	0.09	0.03	13	4.4	11,400 (970)	12,500 (350)	1.2 (0.1)	3900 (490)	4500 (460)	3.3 (0.2)
	6.5	1.27	0.04	180	4.8	1600 (30)	2200 (80)	6.5 (0.2)	860 (50)	890 (100)	15 (2)
	6.2	0	2.62	—	290	—	—	—	430 (70)	530 (120)	23 (4)
	6.5	0.10	3.05	15	350	4600 (290)	6600 (930)	2.3 (0.4)	510 (10)	650 (30)	19 (1)

Clay	pH	C_{init} (Lu)	C_{init} (La)	C_{sorb} (Lu)	C_{sorb} (La)	Lu			La		
						K_d	$K_{d,des}$	R_{des}	K_d	$K_{d,des}$	R_{des}
	6.6	1.24	2.97	170	340	1400 (100)	2000 (70)	7.3 (0.3)	450 (20)	560 (40)	22 (1)
	6.6	3.12	2.93	420	320	1200 (50)	1900 (190)	7.6 (0.5)	390 (20)	470 (9)	25 (1)
	6.3	9.19	2.94	1100	290	660 (20)	1300 (1)	10 (1)	290 (10)	340 (2)	31 (1)

Table 7

Table 7. Changes in the K_d of the Ln (1) due to changes in the concentration of the Ln (2): ratio values of K_d of Ln (1) at varying concentrations of the Ln (2).

C_{init} (Ln (1)) meq L ⁻¹	C_{init} (Ln (2)) meq L ⁻¹	Ratio values of K_d (Ln (1))			
		FEBEX	HEC	MX80	SCa-3
Water medium					
1:La; 2:Lu					
0.09	0.03	1.6	1.9	1.5	1.2
	3				
1	0.03	1.6	1.6	1.0	1.3
	3				
0.03	0	0.9	1.8	1.0	1.4
	0.03				
3	0	1.3	21	1.9	1.1
	3				
1:Lu; 2:La					
0.09	0.03	1.9	1.2	1.3	1.3
	3				
1	0.03	1.1	1.4	1.3	1.3
	3				
0.03	0	1.0	1.2	1.0	1.6
	0.03				
3	0	1.2	6.7	1.4	2.5
	3				
Ca medium					
1:La; 2:Lu					
0.09	0.03	2.6	6.5	22	5.1
	3				
1	0.03	1.9	1.9	1.7	1.9
	3				
0.03	0	2.1	1.3	1.3	3.4
	0.03				
3	0	2.9	4.4	3.0	1.1
	3				
1:Lu; 2:La					
0.09	0.03	1.6	1.0	1.3	2.5

C_{init} (Ln (1)) meq L ⁻¹	C_{init} (Ln (2)) meq L ⁻¹	Ratio values of K_d (Ln (1))			
		FEBEX	HEC	MX80	SCa-3
	3				
1	0.03	1.1	1.1	1.6	1.1
	3				
0.03	0	2.1	1.5	0.7	0.8
	0.03				
3	0	2.0	0.9	0.7	0.7
	3				

Table 8

Table 8. Fitting parameters derived from the Langmuir model. b_1 (meq kg⁻¹), K_1 and K_2 (meq L⁻¹). (Ln (1): prediction of C_{sorb} (1)).

	b_1	K_1	K_2
<i>FEBEX</i>			
Water medium			
La(1); Lu(2)	1150	29	24
Lu(1); La(2)	1056	26	21
Ca medium			
La(1); Lu(2)	942	0.5	0.3
Lu(1); La(2)	2719	0.3	0.2
<i>HEC</i>			
Water medium			
La(1); Lu(2)	662	133	53
Lu(1); La(2)	864	15	7.0
Ca medium			
La(1); Lu(2)	647	0.6	1.9
Lu(1); La(2)	1833	1.0	0.4
<i>MX80</i>			
Water medium			
La(1); Lu(2)	872	13	10
Lu(1); La(2)	988	5.5	4.1
Ca medium			
La(1); Lu(2)	772	0.8	1.8
Lu(1); La(2)	2412	0.4	0.2
<i>SCa-3</i>			
Water medium			
La(1); Lu(2)	1301	16	14
Lu(1); La(2)	1280	29	21
Ca medium			
La(1); Lu(2)	1062	0.6	0.4
Lu(1); La(2)	2101	0.8	0.2

Figure 1

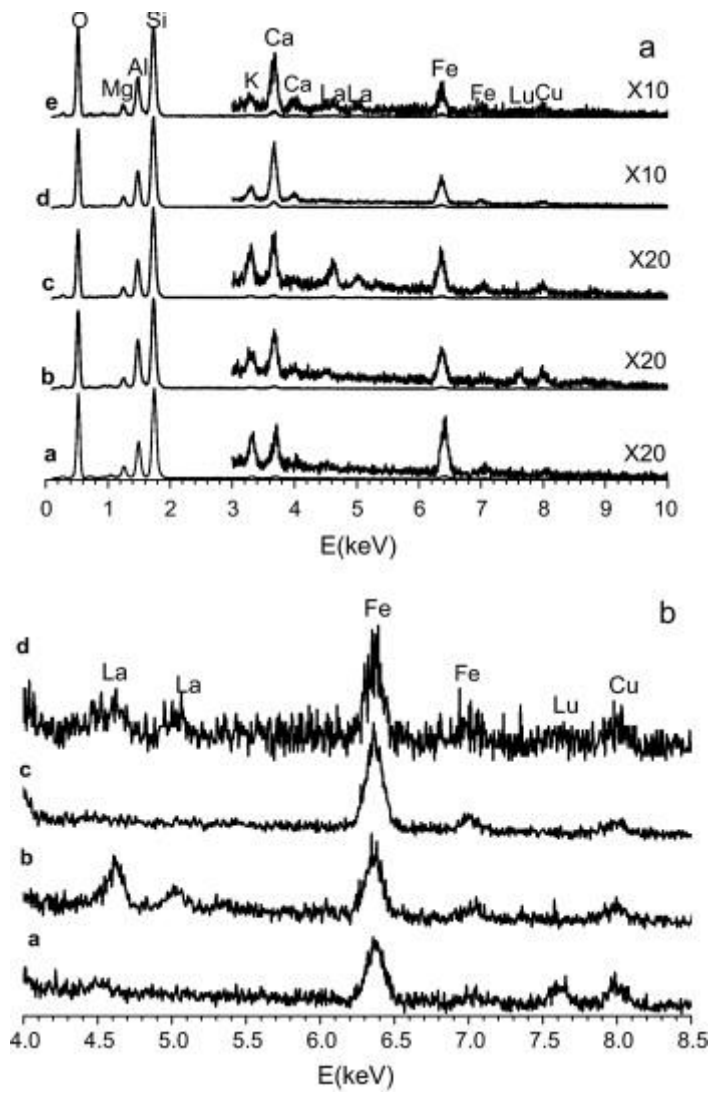


Figure 2

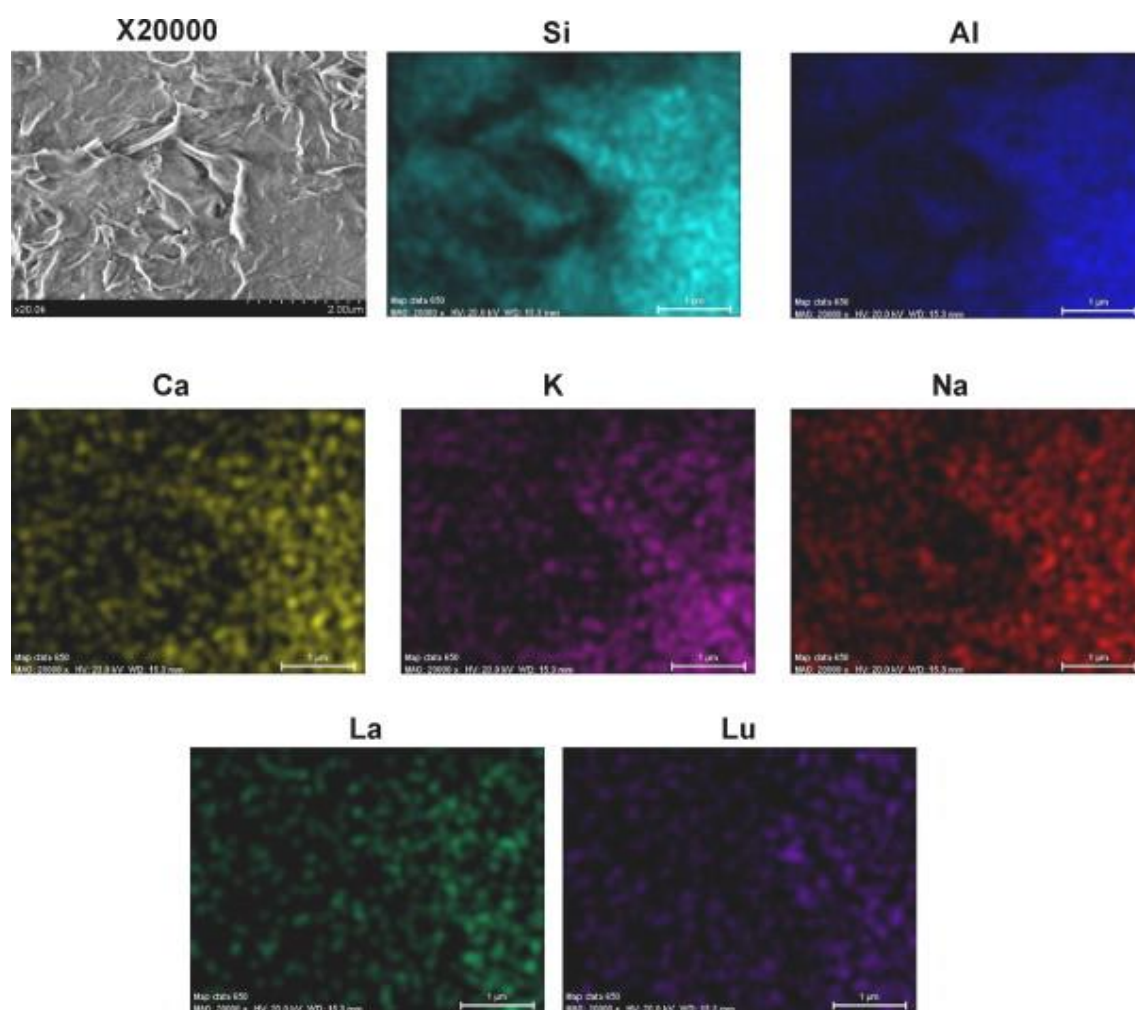


Figure 3

